Pharm Res (2013) 30:342–351
DOI 10.1007/s11095-012-0874-6

RESEARCH PAPER

Effect of PEGylation on Biodistribution and Gene Silencing of siRNA/Lipid Nanoparticle Complexes

Yanjie Bao • Yi Jin • Padmanabh Chivukula • Jun Zhang • Yun Liu • Jian Liu • Jean-Pierre Clamme • Ram I. Mahato • Dominic Ng • Wenbin Ying • Yiting Wang • Lei Yu

Received: 15 May 2012 / Accepted: 23 August 2012 / Published online: 15 September 2012

ABSTRACT

Purpose To determine the influence of physicochemical properties of lipid nanoparticles (LNPs) carrying siRNA on their gene silencing *in vivo*. Mechanistic understanding of how the architecture of the nanoparticle can alter gene expression has also been studied.

Methods The effect of 3-N-[(ω-methoxypoly(ethylene glycol)2000)carbamoyl]-1,2-dimyristyloxy-propylamine (PEG-C-DMA) on hepatic distribution and FVII gene silencing was determined. FVII mRNA in hepatocytes and liver tissues was determined by Q-PCR. Hepatic distribution was quantified by FACS analysis using Cy5 labeled siRNA.

Results Gene silencing was highly dependent on the amount of PEG-C-DMA present. FVII gene silencing inversely correlated to the amount of PEG-C-DMA in LNPs. High FVII gene silencing was obtained *in vitro* and *in vivo* when the molar ratio of PEG-C-DMA to lipid was 0.5 mol%. Surprisingly, PEGylation didn't alter the hepatic distribution of the LNPs at 5 h post administration. Instead the amount of PEG present in the LNPs has an effect on red blood cell disruption at low pH.

Conclusion Low but sufficient PEG-C-DMA amount in LNPs plays an important role for efficient FVII gene silencing *in vivo*. PEGylation did not alter the hepatic distribution of LNPs, but altered gene silencing efficacy by potentially reducing endosomal disruption.

KEY WORDS endosomal disruption · FVII · gene silencing · hepatic distribution · LNP · PEG-C-DMA

INTRODUCTION

Since post-transcriptional gene silencing by RNA interference (RNAi) was first observed in plants in 1990 (1) and its mechanism through double stranded RNA was revealed by Fire *et al.* in 1998 (2), RNAi has been developed into a promising new approach for therapeutics of various diseases (3). Several strategies have been developed to trigger target mRNA degradation, resulting in the inhibition of target protein synthesis. These include i) siRNA, ii) precursor double-stranded RNA (dsRNA) and iii) small hairpin RNA (shRNA) expressing plasmids (3–9). The potential of RNAi is currently being realized as a unique drug entity to specifically reduce the expression of disease causing genes.

siRNA delivery has made considerable progress in the recent years, in addition their relatively ease of chemical synthesis and the lower probability of non-specific side effects has opened a new era of therapeutics molecules (4,8). Several research groups have demonstrated high *in vivo* gene silencing, well-tolerated safety profile and reproducibility of LNPs (4,5). This has led to the initiation of

Y. Bao • Y. Wang (✉) • L. Yu
Biomedical Engineering and Technology Institute
Institutes for Advanced Interdisciplinary Research
East China Normal University
3663 North Zhongshan Road
Shanghai 200062, China
e-mail: ytwang@nbic.ecnu.edu.cn

Y. Bao • Y. Jin • P. Chivukula • J. Zhang • Y. Liu • J. Liu • J.-P. Clamme • D. Ng • W. Ying • L. Yu (✉)
Nitto Denko Technical Corporation
501 Via Del Monte
Oceanside, California 92058, USA
e-mail: ndt.ecnu@gmail.com

R. I. Mahato
Department of Pharmaceutical Sciences
University of Tennessee Health Science Center
19 S Manassas Street
Memphis, Tennessee 38103, USA

various clinical trials, and has rapidly become one of the promising RNAi delivery systems (3). LNPs like other delivery technologies have to overcome several biological barriers of nucleic acid therapy. These include stability in serum, accumulation in target organ and cells, and endosomal release of siRNA in the cytoplasm. One of the key factors to realize the clinical benefit of *in vivo* gene silencing is the ability of siRNA formulations to remain relatively inert during the circulation. To this end, the various polymers have been utilized to shield the nanoparticles from being recognized by the innate immune system.

Hydrophilic polymer namely polyethylene glycol (PEG) is a commonly used excipient to increase the *in vivo* stability, evading recognition by the reticuloendothelial system (RES), prolonging circulation half-life and reducing immunogenicity (10–12). Variations in PEGylation, regarding PEG molecular weights, linear or branched structures, conjugations and incorporation ratios are known to induce changes in particle size and surface morphology, surface charge and other physicochemical properties of liposomes. These physicochemical properties may in turn affect the pharmacokinetic and pharmacodynamic properties of liposome as well as the intracellular performance of siRNA, resulting in an overall change in efficacy (13–19).

Earlier work by Heyes *et al.* has shown that the presence of PEG can alter the gene expression profile of a given carrier (20). This effect has been attributed to the intracellular delivery and trafficking of non-viral vectors in the presence of a PEG shield. Various novel strategies were implemented to ensure that the presence of PEG is transient. Heyes *et al.* have shown that the size of their lipid anchors on the PEG-lipid during the formulation process plays a key role in determining its potency *in vivo*.

Various inconsistencies exist in the literature regarding the amount of PEG-lipid required for optimal *in vivo* gene expression or silencing (21–23). To our knowledge there is no systematic evaluation of how molar content of PEG lipid plays a role *in vitro* and *in vivo*. To this end, we systematically evaluated the effect of PEG-C-DMA on gene silencing efficiency of LNPs *in vitro* and *in vivo* after systemic administration in mice. The mechanistic understanding of how PEG alters gene expression *in vivo* has also been addressed (24).

MATERIALS AND METHODS

Materials

3-*N*-[(ω-Methoxypoly(ethylene-glycol)2000)carbamoyl]-1,2-dimyristyloxy-propylamine (PEG-C-DMA) (average molecular weight of 2500 g/mol) and 1,2-dilinoleyloxy-N,N-dimethyl-3-aminopropane (DLinDMA) (MW=616 g/mol) were synthesized as described previously (20,24). 1,2-distearoyl-*sn*-glycero-3-phosphocholine (DSPC) (MW=790 g/mol) and cholesterol (MW=387 g/mol) were purchased from Avanti Polar Lipids (Alabaster, AL). All siRNAs were synthesized by Nitto Denko Technical Corporation and were characterized by electrospray mass spectrometry and anion exchange high-performance liquid chromatography (HPLC). The sequences for the sense and antisense strands of Factor VII siRNA (abbreviated as siFVII) and control siRNAs have been reported (25): For siFVII, 5′-GGA**uc**A**ucuc**AAG**ucuu**A**c**T*T-3′ was used as a sense strand and 5′-G**u**AAGA**cuu**GAGA**u**GA**ucc**T*T-3′ as an antisense strand. For control siCont, 5′-CUUACGCUGAGUACUU CGAT*T-3′ was used as a sense strand and 5′-UCGAAGUA-CUCAGCGUAAGT*T-3′ as an antisense strand. 2′-Fluoro-modified nucleotides are in bold lower case, and phosphorothioate linkages are represented by asterisks. siRNAs were generated by annealing equimolar amounts of complementary sense and antisense strands. Cy5 labeled at 5′ sense siRNA was used for hepatic distribution study. The Cy5 labeled siRNA was synthesized on the solid support using Cy5-Phosphoramidite (Glen Research, Sterling, VA). Standard coupling conditions for synthesis of Cy5 labeled was carried out at the 5′-end, which formed a phosphodiester linkages. 30 kDa MWCO dialysis tubes were purchased from Spectrum Laboratories, Inc (Rancho Dominguez, CA). 30 kDa MWCO Amicon Ultra-15 Centrifugal Filter Units were purchased from Millipore (Temecula, CA). 2-(N-morpholino) ethanesulfonic acid (MES) buffer, Hank's balance salt solution, liver perfusion media, liver digest media, William's E media, hepatocyte wash media and Quant-iT™ RiboGreen® RNA Reagent and Kit were purchased from Invitrogen (Carlsbad, CA). Percoll™ was purchased from GE Healthcare Life Science (Piscataway, NJ). Nycodenz® was purchased from PROGEN Biotechnik GmbH (Heidelberg, Germany). EGTA, TritonX-100, collagen I, collagenase were purchased from Sigma (St Louis, MO). Anti-mouse PE-CD31 and PE-F4-80 antibodies were purchased from Biolegend (San Diego, CA). QIAshredder, RNeasy Mini Kit and RNAlater RNA Stabilization Reagent were purchased from Qiagen (Valencia, CA). High-Capacity cDNA Reverse Transcription Kit and Power SYBR® Green Master Mix were purchased from Applied Biosystems (Foster City, CA). Mouse FVII and GAPDH primers were customized from Integrated DNA Technologies (Coralville, Iowa). FLx800 Microplate reader was from Biotek Instruments (Winooski, VT). BD Accuri C6 flow cytometer was from BD Accuri Cytometers (Ann Arbor, MI). Gene Amp PCR system 9700 and 7900HT Fast Real-Time PCR System were from Applied Biosystem (Life Technologies Corporation, Carlsbad, CA). Zetasizer Nano ZS was from Malvern (UK).

Animal Studies

Six to eight week old C57BL/6 mice and 200 g SD rats were purchased from Charles River Laboratories

(Wilmington, MA). All procedures used in animal studies were conducted at University of California-San Diego, approved by the Institutional Animal Care and Use Committee (IACUC) and complied with local, state, and federal regulations as applicable.

Lipid Nanoparticle (LNP) Formulation

LNPs were formulated as described by Jeffs *et al.* (26) and MacLachlan *et al.* (27). The composition for LNPs was PEG-C-DMA: DLinDMA: Cholesterol: DSPC in a mole percent ratio of x: 40: (50-x): 10 (x=0.1, 0.5, 1, 2, 5, 8, and 10). The charge ratio of cationic lipid to siRNA was 7.60, while the total lipid concentration was 27.76 mM. Brief procedure for particle formation is as follows: lipids were dissolved in ethanol, anti-FVII siRNA, siCont siRNA and Cy5 labeled siRNA were dissolved in citrate buffer. The lipid solution and siRNA solution were mixed with a 100 ml/min flow rate at 37°C. After mixing, the two solutions were diluted with citrate-NaCl buffer with the flow rate of 200 ml/min. Both mixing and dilution steps were conducted in a T-connector with the bore size 1/16 inch. This solution was allowed to return to ambient temperature. Subsequently, the nanoparticles were then dialyzed with 30 kDa MWCO dialysis tube in PBS and then concentrated by 30 kDa MWCO Amicon Ultra-15 Centrifugal Filter Units.

LNP Characterization

Mean particle size, polydispersity index (PDI) and zeta potential (ζ) of siFVII LNPs formulated with different PEG-C-DMA contents were determined by Dynamic Light Scattering (DLS) using Zetasizer Nano ZS (Malvern, UK). LNPs were diluted in 0.01 M PBS (pH=7.4) for measurement. Each sample was measured in triplicate. Mean particle size and standard deviation were calculated. The quantification of PEG lipid was also done with an Acquity UPLC system (Waters Corporation) equipped with an evaporative light-scattering detection (ELSD). LNP formulation was injected onto a 1.7 μm particle 50×2.1 mm id waters acquity BEH C-18 column (Waters); the column was maintained at 55°C for the lipid analysis. The flow rate used for these experiments was 0.6 ml/min. A binary gradient system was used.

siRNA Recovery Efficiency and Encapsulation Efficiency Measurement

siRNA recovery efficiency (R.E.) and encapsulation efficiency (E.E.) of LNPs were determined by RiboGreen assay using Quant-iT™ RiboGreen® RNA Reagent and Kit as described by the manufacturer. Briefly, LNPs were diluted and destabilized by treating with 1% Triton-X100 for 30 min for total siRNA measurement. The free siRNA amount was measured directly without Triton-X addition.

$$\mathrm{RE} = \text{total siRNA amount}/\text{feeding siRNA amount} \times 100\%$$

$$\mathrm{EE} = (\text{total siRNA amount} - \text{free siRNA amount})$$

$$/\text{total siRNA amount} \times 100\%$$

Each measurement was run in triplicate.

Isolation of Primary Mouse Hepatocytes

Six to eight weeks male C57BL/6 mice were anesthetized using Isoflurane before surgery. Mouse liver was perfused with pre-warmed liver perfusion media and liver digest media, and then incubated in digest media. The digested liver was minced gently and then filtered through 100 μM cell strainer. Gained cells were washed by wash medium and then seeded in collagen I pre-coated 6-well plates (6–10×10^5 cells/well) using Williams E media with 10% FBS+1% antibiotics. After 2–4 h, the cells were washed once with PBS and added fresh medium to remove the floating dead cells. Hepatocytes were identified by using anti-albumin immunofluorescent staining assay.

Transfection of Primary Hepatocytes

Transfection was carried out at 24 h after cell seeding using LNPs (56.6 nM equivalent concentration of siRNA) containing siFVII or siCont with different PEG-C-DMA molar ratio ranging from 0.1% to 10%. Cells in each well were collected at 24 h after transfection. Total RNA was extracted by QIAGEN RNeasy Mini Kit. Reverse transcription was performed using ABI High-Capacity cDNA Reverse Transcription Kit to obtain cDNA products. The power SYBR® Green Master Mix, FVII and GAPDH primers were used for quantitative real-time PCR assay to detect FVII mRNA expression relative to the house keeping gene GAPDH. Each condition was performed in triplicate.

FVII Gene Silencing after Systemic Administration of LNPs into Mice

Six to eight week old male C57BL/6 mice were used for the study. All LNPs were administered under normal pressure via tail vein injection into C57BL/6 mice at a single dose of 3 mg/kg·bw, equivalent amount of siRNA, n=5. Animals had been anesthetized using Isoflurane and heart perfused at 48 h after administration, and then livers were collected and homogenized for RNA extraction. FVII mRNA levels were measured by Q-PCR and normalized to GAPDH mRNA as described above. Each measurement was conducted in triplicate.

Hepatic Distribution in Mice

Six to eight week old male C57BL/6 mice were injected intravenously with Cy5-labeled siRNA LNPs. The injections were administered under normal pressure at a single dose of 2.5 mg/kg equivalent amount of siRNA. At 1 h and 5 h after the injection, hepatocytes and non-parenchyma cells (including Kupffer cells, hepatic stellate cells and endothelial cells) fractions of mouse livers were obtained by the collagenase method described before (28,29). Briefly, the livers were perfused with Hank's Balanced Salt Solution (HBSS), EGTA HBSS and followed by 0.03% collagenase HBSS at 37°C for 20 min. The perfused livers were incubated in 0.03% collagenase and 0.001% DNAase at 37°C for 20 min and then gently homogenized and filtered through 100 μM cell strainer. Nycodenz solution was then added to the supernatant to make 11% Nycodenz gradient. After centrifugation, non-parenchyma cell fraction (Kupffer cells, hepatic stellate cells and endothelial cells) and hepatocyte-rich fraction were obtained. Non-parenchymal cell fraction was then incubated with fluorescent labeled antibodies to separate and identify Kupffer cells (anti-mouse PE- F4/80) and endothelial cells (anti-mouse PE-CD31) separately by flow cytometer. Non-parenchyma cell fraction was also fixed with 4% PFA and treated by TritonX 100- Tween 20 and then incubated with Desmin to confirm hepatic stellate cell population. Hepatocyte-rich fraction was then washed and added to 60% percoll to make 30% percoll gradient for hepatocyte separation by centrifugation, and then analyzed by flow cytometer. Only propidium iodide negative hepatocytes were counted. Mean fluorescent intensity (MFI) of Cy5 signal of different cell types was determined and analyzed by flow cytometer. Each experiment was carried out on 3 different mice on 3 different days. Mean and standard deviation were calculated.

Hemolysis Assays

SD rat red blood cells (RBCs) were selected as the endosomal membrane model to investigate the endosome disrupting ability of LNPs formulated with different PEG-C-DMA molar ratios. The RBC disruption was performed as described before (30,31). Briefly, blood sample was collected freshly in a sodium citrate rinsed tube. RBCs were harvested after centrifugation at 3000 rpm for 10 min and then rinsed with D-PBS (pH 7.4) 3 times until the supernatant became clear. RBCs were counted with a hemacytometer and diluted either in isotonic phosphate or 2-(*N*-morpholino) ethanesulfonic acid (MES, 200 mM, NaCl 110 mM) buffer of the appropriate pH (pH7.4 and pH5.5, respectively). The LNPs were adjusted to appropriate concentration by D-PBS (pH 7.4) and then added to RBC solutions (final cell concentration=5×10^7 RBC/ml). The samples were incubated for 30 min at 37°C on a 3-D rotation station. Centrifugation was carried out after the incubation, and the hemoglobin absorbance in the supernatant was measured at 541 nm to determine the extent of membrane disruption. To obtain 100% hemolysis, cells were treated with 0.2% Triton X-100. Data were presented as average of % related to 0.2% Triton X-100 treated samples. Each measurement was conducted in triplicate. Mean and standard deviation were calculated.

Statistical Analyses

Independent sample t-test was carried out using excel 2007 (Microsoft). All the data were presented as a mean value with its standard deviation indicated (mean ± S.D.). The means were judged to be significantly different when $P<0.05$ and highly significantly different when $P<0.01$ or $P<0.001$.

RESULTS

LNP Formulation with Different PEG-C-DMA Molar Ratios

To investigate how PEG-C-DMA molar ratio affects LNPs on silencing FVII gene *in vitro* and *in vivo*, siFVII LNPs with 7 different PEG-C-DMA molar ratios were formulated with the following lipid compositions: PEG-C-DMA : DLinDMA : cholesterol : DSPC=x : 40 : (50-x) : 10 (x=0.1, 0.5, 1, 2, 5, 8, 10). The N/P ratio of the formulation was kept constant at 7.60.

Physicochemical Characterization

Mean particle size (Z-ave), PDI and ζ potential of LNPs were determined by dynamic light scattering (DLS) and were summarized in Table I. Each LNP sample was monitored twice: the first measurement was right after the dilution step with citrate-NaCl buffer, while the second measurement was for the final product after all processes.

Table I Mean Particle Size, Polydispersity Index (PDI) and ζ Potential of siFVII LNPs Formulated with Different PEG-C-DMA Molar Ratios

PEG-C-DMA (mole%)	Mean particle size (nm)	PDI	ZP (mV)
0.5	132 ± 1	0.051 ± 0.008	0.3 ± 4.0
1	103 ± 1	0.093 ± 0.013	0.9 ± 0.7
2	86 ± 1	0.115 ± 0.022	−0.5 ± 1.8
5	86 ± 1	0.161 ± 0.006	−0.8 ± 1.3
8	74 ± 1	0.236 ± 0.011	−0.9 ± 1.1
10	65 ± 1	0.193 ± 0.006	−0.4 ± 0.9

LNPs were diluted in PBS (pH=7.4) for the measurement. There was no significant difference in the mean particle size before and after the dilution step for the same LNP sample except the one formulated with 0.1 mole% PEG-C-DMA, which indicated that the LNPs were stable during the dialysis and concentration process. The same physical properties were obtained for the LNPs using control siRNA and Cy5-siRNA sequence. The PEG-C-DMA content was quantified using an Acquity UPLC system. We observed very good correlation with the feed ratio and the amount of PEG incorporated into the LNP formulations (Table II). Typically, we observed an incorporation of approximately 80% of the feed ratio.

LNPs formulated with 0.1 mole % PEG-C-DMA were not stable, in which aggregation and stratification were observed during the formulation process. The mean particle size of 0.1 mole% PEG-C-DMA LNPs was around 2000 nm (2067 ± 61 nm for siFVII LNPs), and a large PDI (indicating a very wide particle size distribution). Therefore, 0.1 mole% PEG-C-DMA was not used for further evaluation. The mean particle size of 65–132 nm of siFVII LNPs formulated with PEG-C-DMA molar ratio ranging from 0.5% to 10% matched the criterion for avoiding capture by Kupffer cells, and these LNPs can diffuse out of the sinusoids through the fenestrations and reach the hepatocytes (Table I) (32). PDI shows the distribution of individual molecular masses in a LNP sample, low PDI indicates a narrow particle size distribution. The PDIs of LNPs formulated with PEG-C-DMA molar ratio ranging from 0.5% to 10% were low (0.051–0.236 for siFVII LNPs) with a slightly increasing trend (Table I). This indicated that when the PEG-C-DMA molar ratio was ≥0.5 mole%, increasing PEG-C-DMA molar ratio led to the formation of LNPs with a slightly broader size distribution.

ζ potential represents the surface charge of liposome particles. As shown in Table I, ζ potential of siFVII LNPs was in the range of - 0.9 and 0.9 mV, which is close to neutral and decreased only slightly when PEG-C-DMA molar ratio was increased from 0.5% to 10%. We also looked at shelf-life stability of LNP particles at 4 ^{0}C for up to a year (Table III). This indicated that when the PEG-C-DMA molar ratio was ≥0.5 mole% the particles were stable without aggregation for up to one year as measured by no change in particle size.

Table II Quantification of PEG Lipids Encapsulated in LNP

PEG-C-DMA Feed ratio (mole%)	PEG-C-DMA Measured ratio (%)	Revovery Yield (%)
0.5	0.40	78.9
1	0.62	62.2
2	1.65	82.4
10	7.82	78.2

Table III One Year Stability of LNP Particles at 4°C

	antiFVII siRNA			
PEG-C-DMA (mole%)	Mean particle size (nm) *T*=0	PDI	Mean particle size (nm) *T*= 1 year	PDI
0.5	132.3	0.051	132.0	0.043
1	102.6	0.093	101.6	0.070
2	86.1	0.115	84.5	0.107
5	86.0	0.161	82.3	0.150
8	73.6	0.236	67.2	0.219
10	64.6	0.193	60.9	0.166
0.1	2067.3	0.983	1561.7	0.877

siRNA Recovery Efficiency and Encapsulation Efficiency

Recovery efficiency (RE) was calculated by measuring siRNA concentration before and after the formulation process. As shown in Table IV, when the PEG-C-DMA molar ratio was equal to or below 5.0 mole%, the RE of siFVII LNPs was greater than 85%. When PEG content was 5.0 mole%, LNPs showed the maximum RE of 97%. Lowering the molar ratio of PEG slightly decreased the recovery (0.5 mole % PEG-C-DMA LNPs had a RE of 85%). When the PEG-C-DMA molar ratio was 8 and 10%, the RE dropped to 76 and 79%, respectively. There was no significant difference among LNPs formulated with different siRNA sequence. Encapsulation efficiency (EE) is an indicator of the amount of ribogreen accessible siRNA present. The EE of anti-FVII siRNA LNPs formulated with PEG-C-DMA molar ratio ranging from 0.5–10 mole % was around 88–94 (Table IV). This indicated that the LNP formulation process is quite robust and reproducible.

Table IV siRNA Recovery Efficiency (RE) and Encapsulation Efficiency (EE) of siFVII LNPs Formulated with Different PEG-C-DMA Molar Ratios

PEG-C-DMA (mole%)	Recovery efficiency (%)	Encapsulation efficiency (%)
0.5	85 ± 1	88
1	93 ± 1	92
2	90 ± 1	93
5	97 ± 1	92
8	76 ± 1	91
10	79 ± 1	94

Effect of PEG-C-DMA in LNPs on FVII Gene Silencing *In Vitro*

To determine the effect of PEG-C-DMA mole percent ratio in LNPs on FVII gene silencing *in vitro*, we isolated primary hepatocytes from 6–8 week old C57BL/6 mice. Obtained mouse hepatocytes showed a normal morphology with polygonal cells and frequently had two or more nuclei per cell. More than 90% of cells were stained positive for albumin (a marker for hepatocytes) by immunofluorescence (data not shown). Transfections by LNPs formulated with different PEG-C-DMA molar ratio ranging from 0.5% to 10% were carried out at 24 h after cell seeding, and each condition was repeated in triplicate (control siRNA was also tested using the same condition). The LNPs were incubated with the cells for 24 h, total RNA was extracted, reverse transcribed, and the cDNA product was used for quantitative real-time PCR (Q-PCR) assay to determine FVII mRNA expression relative to the house keeping gene GAPDH. Q-PCR for each cDNA product was performed in triplicate.

As shown in Fig. 1, FVII gene of primary mouse hepatocytes was highly significantly silenced (**, $P<0.01$, compared to non-treatment group by t-test.) by 0.5–2.0 mole% PEG-C-DMA siFVII LNPs or significantly silenced (*, $P<0.05$, compared to non-treatment group by t-test) by 5–10 mole% PEG-C-DMA siFVII LNPs with a decreasing silencing efficacy from 99.3±0.5 (0.5 mole% PEG-C-DMA siFVII LNPs) to 62.6±3.2% (10 mole% PEG-C-DMA siFVII RNA LNPs). The LNPs formulated with siCont showed negligible knockdown.

Effect of PEG-C-DMA in LNPs on FVII Gene Silencing *In Vivo*

FVII gene silencing study on C57BL/6 mice was conducted using the formulated LNPs. Livers were collected and homogenized for RNA extraction 48 h after a single intravenous (i.v.) administration of LNPs at the dose of (3 mg/kg·bw, equivalent amount of siRNA, $n=5$). Animals were anesthetized and heart perfused before organ collection. FVII mRNA levels were determined by Q-PCR (in triplicate) and normalized to GAPDH mRNA. As shown in Fig. 2, the FVII gene in mice liver was silenced from 89.0 ±6.4% (0.5 mole% PEG-C-DMA anti-FVII siRNA LNPs) to 17.9±16.4% (10 mole% PEG-C-DMA anti-FVII siRNA LNPs) by anti-FVII siRNA LNPs ($P<0.01$ for 10 mole% PEG-C-DMA anti-FVII LNPs; $P<0.001$ for other anti-FVII LNPs compared to PBS treated mice group by t-test.). The FVII gene silencing efficacies were inversely correlated to PEG-C-DMA molar ratios in anti-FVII siRNA LNPs; these results were similar to what was observed *in vitro*. To ensure specific silencing due to targeted antisense down regulation, non-specific siRNA was also tested in conjunction. The non-specific sequence showed negligible knockdown, suggesting a specific dicer related interference.

Hepatic Distribution in Mice

It is well known that PEG molar ratio in LNPs can have dramatic impact on the intravascular half-life of nanoparticles (19). Decorating hydrophilic polymers like PEG to the outer surface of nanoparticles prevents opsonization, thereby reducing clearance by RES (13,33). PEG concentration can dramatically impact the pharmacokinetics and ultimately the extravasation to target organs. It is however not

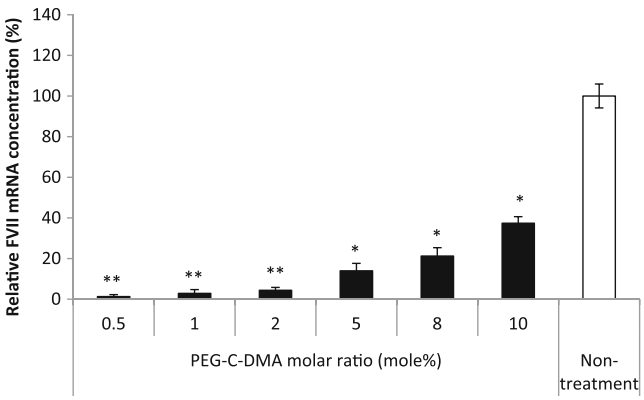

Fig. 1 FVII mRNA silencing in primary mouse hepatocytes using siFVII LNPs formulated with different PEG-C-DMA molar ratios. FVII mRNA levels of primary mouse hepatocytes normalized to GAPDH mRNA were determined by Q-PCR 24 h after transfection (56.6 nM equivalent concentration of siRNA, triplicates per sample.*, $P<0.05$; **, $P<0.01$; compared to non-treatment group by t-test. Results are represented was the mean ± S.D. ($n=3$).

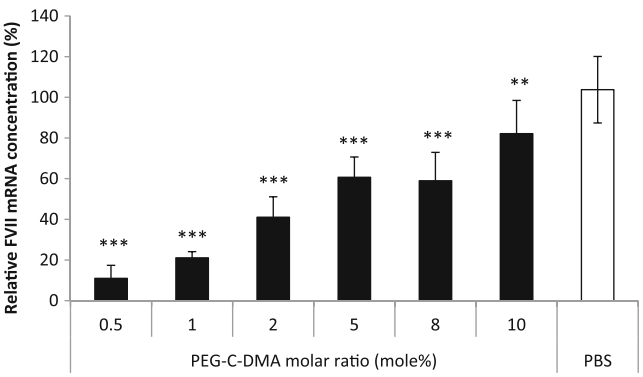

Fig. 2 FVII mRNA silencing in mice (C57BL/6) using siFVII LNPs formulated with different PEG-C-DMA molar ratios. Livers were collected 48 h after intravenous injection at the dose of 3 mg/kg (equivalent amount of siRNA, single dose). FVII mRNA levels of liver homogenates were normalized to GAPDH mRNA and determined by Q-PCR. (**, $P<0.01$; ***, $P<0.001$ compared to PBS mice group by t-test. Results are represented was the mean ± S.D. ($n=5$).

well known if PEGylation hinders the intracellular distribution within the liver.

Liver intracellular distribution of Cy5 labeled LNPs formulated with 0.5, 1, 2, 10 mole% PEG-C-DMA were investigated. At one hour after intravenous injection, mean fluorescence intensity (MFI) of Cy5 signal on hepatocytes from mice treated with Cy5-labeled siRNA LNPs formulated with 0.5 mole% PEG-C-DMA was the lowest and that of 10 mole% was the highest (Fig. 3a). The MFI of hepatocytes treated with10 mole% PEG-C-DMA LNPs was 5.7 times over the ones treated with 0.5 mole% PEG-C-DMA LNPs, an inverse correlation of PEG on the hepatocyte uptake and gene silencing at the initial time points. However, at 5 hours after administration, all MFIs of hepatocytes dropped down to similar level (Fig. 3a) with no significant difference among hepatocytes of mice treated with LNPs formulated with different PEG-C-DMA molar ratios. This suggests the *in vivo* knockdown of Factor VII is not due to an altered intracellular distribution.

The MFI of Kupffer cells uptake at 1 hour after administration was correlated to the PEG-C-DMA molar ratio in LNPs, increasing the PEG content reduced macrophage uptake (Fig. 3b). At 5 h after administration, MFI of Kupffer cells treated with 0.5 mole% PEG-C-DMA Cy5-labeled siRNA LNPs was 1.5 times that of 1 h post administration. The uptake of Kupffer cells treated with 1 mole% PEG remained the same at both time points, but ones treated with 2 mole% and 10 mole% was 34% and 18% compared to its 1 h post administration respectively (Fig. 3b). These data suggest that with less PEG-C-DMA, LNPs were easier to be taken up by Kupffer cells possibly through an opsonization mechanism. This also correlates with reduced hepatocyte uptake of the LNPs with less PEG.

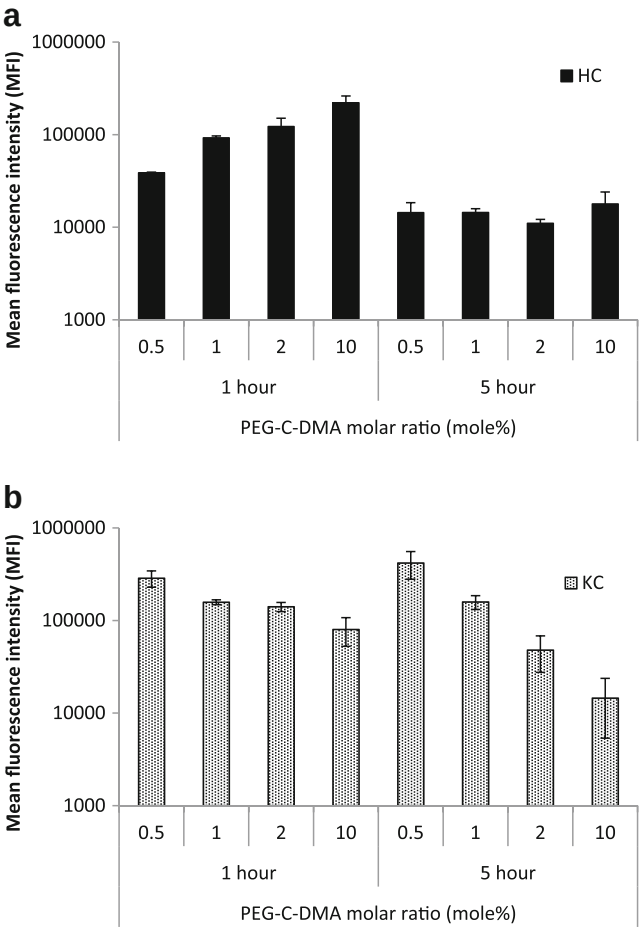

Fig. 3 Hepatic distribution of Cy5-labeled siRNA LNPs formulated with different PEG-C-DMA molar ratios after systemic administration in C57BL/6 mice. Livers were collected at 1 h or 5 h after intravenous injection at the dose of 2.5 mg/kg (equivalent amount of siRNA, single dose). Hepatocytes (HC) and non-parenchymal cells from mice were isolated by Nycodenz gradient. Mean fluorescence intensity (MFI) of Cy5 signal on hepatocytes or Kupffer cells (KC) was determined by flow cytometer with a 640 nm excitation wavelength and 675 nm emission detection afterwards. The fluorescence was corrected for the auto fluorescence of the given cell type, respectively. (**a**) Logarithmic scale MFI of hepatocytes. Only live hepatocytes were counted, separated by propidium iodide. (**b**) Logarithmic scale of MFI of Kupffer cells. Only F4/80 antibody positive Kupffer cells were counted. Results are represented was the mean ± S.D. (n=3).

Hemolysis Assays

Hemolysis was used to determine the potential endosomolytic activity of the LNPs. At pH 7.4, hemolysis was observed for LNPs formulated with 0.5, 1, 2, 10 mole% PEG-C-DMA (2% to 30% RBC hemolysis), while substantial pH-dependent hemolytic activity was evident when the pH was reduced (21% to 90% RBC hemolysis ability at pH 5.5). Interestingly, RBC hemolysis abilities at both pHs were inversely correlated to PEG-C-DMA molar ratio in LNPs (Fig. 4). At pH 5.5, the PEG-C-DMA molar ratios played a significant role in the extent of hemolytic activity. LNPs

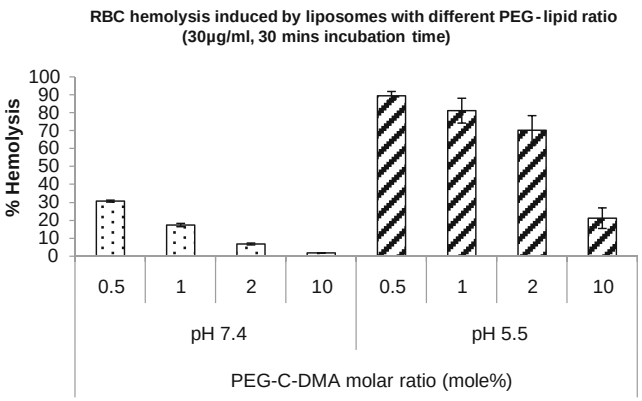

Fig. 4 RBC hemolysis induced by siRNA LNPs formulated with different PEG-C-DMA molar ratios at 37°C at pH 7.4 (dots) or pH 5.5 (diagonal stripes), was determined after 30 min incubation by the absorbance of released hemoglobin at 541 nm. RBCs suspended in PBS (pH 7.4) or MES buffer (pH 5.5), were added to LNPs (30 μg/ml, equivalent amount of siRNA) dissolved in the same buffer, respectively. Data was presented as average of % related to positive control - 0.2% triton X-100. (Error bars represent standard deviation, n=3).

formulated with less PEG-C-DMA had better endosome disrupting ability, leading to potentially a better siRNA release ability and high FVII gene silencing efficacy. These results suggest that hemolytic activity of LNPs is tightly linked to its efficacy.

DISCUSSION

Physicochemical properties play an important role in the interaction of cationic LNPs with biological membranes. Although cationic liposomes and polymers are being used for siRNA delivery, little attention has been paid to understanding the effect of their physicochemical characteristics on cellular uptake, hepatic distribution and gene silencing after systemic administration.

A releasable PEG-C_{14} lipid consisting of a 2 kDa PEG segment was designed for quick release from the LNPs after parenteral injection (20,34). Previously, PEG-C-DMA was used in conjunction with the unsaturated ionizable cationic lipids (DLinDMA), which gave LNPs with a desired size range of 130–140 nm and were efficacious *in vivo* (20). The releasable PEG-lipid reported earlier is thought to quickly segregate from the lipid particle after systemic administration. This release was thought to be pivotal for high gene silencing as a rich hydrophilic surface could inhibit uptake of LNP by target cells. The releasable PEG designed is expected to have an intravascular half-life of 1 h.

In this study, we have tried to thoroughly determine the effect of PEGylation in LNPs on FVII gene silencing *in vitro* and *in vivo* and further investigated the potential mechanism of its action. To this end, we varied the mole percent of PEG in LNPs and investigated its knockdown, as well as its effects on physicochemical properties, hepatic distribution and RBC hemolysis to elucidate a potential mechanism.

siFVII LNPs with PEG-C-DMA molar ratio ranging from 0.5% to 10% had a mean particle size in the range of 132 nm to 65 nm, respectively (Table I). Small nanoparticles (<150 nm) can avoid capture by Kupffer cells and can diffuse out of the sinusoids through the fenestrations and reach the hepatocyte (32). Improved delivery to the parenchyma is achieved through much smaller particles as well (≤50 nm) that can diffuse deeper in the perisinusoidal space (35–37). Hence, one would expect enhanced delivery to hepatocyte's for LNPs with a higher PEG content.

Interestingly, increasing PEG-C-DMA molar ratio helped to form smaller LNPs, suggesting a unique process to control LNP size by adjusting PEG-C-DMA molar ratio. Previously, Garbuzenko *et al.* has suggested that changing the molar ratio of 2 kDa polyethylene glycol-disteroylphosphoethanolamine (PEG–DSPE) induced a change in the compressibility and packing parameter of liposomes (17). Increasing PEG–DSPE mol% up to 7 ± 2% led to increased lipid bilayer compressibility resulting in a decreased size, which was also observed by our results. In our study, even the largest formulated LNP was believed to be able to access parenchyma cells through the fenestrated endothelium of C57BL/6 mice (141 ± 5.4 nm) (35). The surface charge of all these LNPs' was close to neutral (Table I, ζ potential=−1 – 1 mV), which was consistent with previous reports (20).

At 48 h after systemic administration, 89.0 ± 6.4% to 17.9 ± 16.4% of FVII gene silencing by siFVII LNPs in C57BL/6 mouse liver were observed. These results seemed to be inversely correlated to PEG-C-DMA molar ratios in LNPs, which was consistent with the results observed *in vitro*. 0.5 mole% PEG-C-DMA had the highest FVII gene silencing *in vitro and in vivo*. Previously reported formulation contained 2 mol% PEG behaved very similar to the LNPs reported here (20). The mean particle sizes of these LNPs varied from 65 nm–132 nm, well within the range of endocytic uptake (38).

Two possible mechanisms for low gene silencing with increased PEG were evaluated, first the change in pharmacokinetics due to PEGylation was studied by evaluating the hepatic distribution and second an altered intra-cellular release was also examined by evaluating its membrane disruption ability.

It was believed that the presence of a PEG-lipid was only required during the formulation process to prevent aggregation. Once the formulation is injected intravenously the PEG-lipid should quickly release siRNA for optimum transfection. To test this hypothesis, a hepatic distribution study was carried out to evaluate if liver parenchymal cell uptake would differ by changing the PEG molar ratio. We observed quick accumulation of LNPs within the hepatocytes one hour after administration (Fig. 3a). Unexpectedly, higher PEG containing nanoparticles seem to be preferentially taken up by the hepatocytes at the initial time points. After 5 h, there was no significant difference in LNP accumulation in hepatocytes treated with different PEG-C-DMA molar ratio. Therefore, we concluded that changes in pharmacokinetics and target cell accumulation of LNPs due to PEG could not explain the difference in *in vivo* gene silencing.

Interestingly, we found greater cellular uptake by Kupffer cells for LNPs formulated with less PEG-C-DMA during the hepatic distribution study (Fig. 3b). Opsonins were believed to involve in liposome uptake by liver macrophages and hepatocytes. Once nanoparticles injected intravenously, liposomes could adsorb a collection of plasma proteins. Depending on liposome characteristics, potentially, the amount of adsorption for each type of protein could vary. One or more of these proteins may interact with specific receptors on the surface of macrophages or hepatocytes and facilitate its clearance (39). Many investigations have suggested that apolipoprotein E (apoE) was a hepatocyte-directed opsonin (39,40), and important in

directing LNPs to hepatocyte. Akinc *et al.* found that apoE also acts as an endogenous targeting ligand for ionizable LNPs (41). Particles containing less PEG intrinsically had a larger particle size, after protein adsorption these nanoparticles would be much larger than it's highly peglyated counterpart. This could potentially lead to an altered protein absorption and faster clearance.

An altered intra-cellular release was also examined next by evaluating its membrane disruption ability. LNPs were formulated with an ionizable cationic lipid DLinDMA with a pK_a of 6.8 (40). RBC hemolysis was used to evaluate the membrane disruption ability of LNPs formulated with 0.5, 1, 2, 10 mole% PEG-C-DMA. The disruption was 21% to 90% at pH 5.5 and inversely proportional to the PEG-C-DMA molar ratio in LNPs (Fig. 4). At pH 7.4, hemolysis was also observed for the LNPs albeit to a lesser degree (2% to 30% RBC hemolysis). The lesser degree of hemolysis at neutral pH was attributed to the lower ionization degree of DLinDMA. When the cationic lipid gets protonated, it causes a nonbilayer (hexagonal H_{II}) phase structure in the presence of the anionic bilayer (40). The extent of RBC hemolysis can be attributed to two parameters, the pKa of the ionizable lipid and the charge shielding effect of PEGylation. Even at physiological pH a substantial amount of ionizable lipid is protonated, thus facilitating interaction with the negative charged RBC membrane and causing disruption. This effect is clearly is more pronounced with the pH is reduced to further protonate the LNPs. PEGylation on the other hand facilitates charge shielding thereby potentially reducing the LNP interaction with RBC membrane. Hence, an inverse correlation with the amount of PEG-lipid and RBC disruption is seen. Particles that contained high molar ratio of PEG significantly attenuated the disruption at both pH, which could be a cause for decreased efficiency of gene silencing with high PEG content in LNPs *in vitro* as well as *in vivo*.

Overall, PEG-C-DMA molar ratio in LNPs affected the extent of FVII gene silencing, and 0.5 mole% PEG-C-DMA was the molar ratio in our study to achieve the highest gene silencing. More importantly, PEG content varied endosome disrupting abilities of formulated LNPs, which could play an important role in its efficacy.

CONCLUSION

In this study, we prepared and characterized LNPs containing varied amount of PEG-C-DMA for siFVII siRNA delivery. LNPs formulated with less PEG-C-DMA had better FVII mRNA silencing both *in vitro* and *in vivo*. 0.5 mole% PEG-C-DMA was the molar ratio to achieve high FVII gene silencing. Contrary to popular belief hepatocyte uptake of LNPs was not inhibited by increasing PEG content. PEG-C-DMA molar ratio however significantly altered the RBC hemolysis at both neutral and acidic pH, and this shift could be crucial for altering gene silencing. Hence, the use of acid sensitive releasable PEG could afford further insight into its mechanism. Often overlooked but crucial parameter is the endosome disrupting ability of nanoparticles formulation. This should be always addressed when designing siRNA nanocarriers.

REFERENCES

1. Napoli C, Lemieux C, Jorgensen R. Introduction of a chimeric chalcone synthase gene into petunia results in reversible co-suppression of homologous genes in trans. Plant Cell. 1990;2(4):279–89.
2. Fire A, Xu S, Montgomery MK, Kostas SA, Driver SE, Mello CC. Potent and specific genetic interference by double-stranded RNA in Caenorhabditis elegans. Nature. 1998;391(6669):806–11.
3. Lares MR, Rossi JJ, Ouellet DL. RNAi and small interfering RNAs in human disease therapeutic applications. Trends Biotechnol. 2010;28(11):570–9.
4. Aagaard L, Rossi JJ. RNAi therapeutics: principles, prospects and challenges. Adv Drug Deliv Rev. 2007;59(2–3):75–86.
5. Bartel DP. MicroRNAs: genomics, biogenesis, mechanism, and function. Cell. 2004;116(2):281–97.
6. De Paula D, Bentley MV, Mahato RI. Hydrophobization and bioconjugation for enhanced siRNA delivery and targeting. RNA. 2007;13(4):431–56.
7. Lu PY, Woodle MC. Delivering small interfering RNA for novel therapeutics. Methods Mol Biol. 2008;437:93–107.
8. Meister G, Tuschl T. Mechanisms of gene silencing by double-stranded RNA. Nature. 2004;431(7006):343–9.
9. Tang G. siRNA and miRNA: an insight into RISCs. Trends Biochem Sci. 2005;30(2):106–14.
10. Chinol M, Casalini P, Maggiolo M, Canevari S, Omodeo ES, Caliceti P, *et al.* Biochemical modifications of avidin improve pharmacokinetics and biodistribution, and reduce immunogenicity. Br J Cancer. 1998;78(2):189–97.
11. Harris JM, Chess RB. Effect of pegylation on pharmaceuticals. Nat Rev Drug Discov. 2003;2(3):214–21.
12. Semple SC, Harasym TO, Clow KA, Ansell SM, Klimuk SK, Hope MJ. Immunogenicity and rapid blood clearance of liposomes containing polyethylene glycol-lipid conjugates and nucleic Acid. J Pharmacol Exp Ther. 2005;312(3):1020–6.
13. Harris JM, Martin NE, Modi M. Pegylation: a novel process for modifying pharmacokinetics. Clin Pharmacokinet. 2001;40(7):539–51.
14. Needham D, Kim DH. PEG-covered lipid surfaces: bilayers and monolayers. Colloids Surf B Biointerfaces. 2000;18(3–4):183–95.
15. Litzinger DC, Buiting AM, van Rooijen N, Huang L. Effect of liposome size on the circulation time and intraorgan distribution of amphipathic poly(ethylene glycol)-containing liposomes. Biochim Biophys Acta. 1994;1190(1):99–107.
16. Dan N. Effect of liposome charge and PEG polymer layer thickness on cell-liposome electrostatic interactions. Biochim Biophys Acta. 2002;1564(2):343–8.
17. Garbuzenko O, Barenholz Y, Priev A. Effect of grafted PEG on liposome size and on compressibility and packing of lipid bilayer. Chem Phys Lipids. 2005;135(2):117–29.
18. Reddy KR. Controlled-release, pegylation, liposomal formulations: new mechanisms in the delivery of injectable drugs. Ann Pharmacother. 2000;34(7–8):915–23.

19. Klibanov AL, Maruyama K, Torchilin VP, Huang L. Amphipathic polyethyleneglycols effectively prolong the circulation time of liposomes. FEBS Lett. 1990;268(1):235–7.
20. Heyes J, Palmer L, Bremner K, MacLachlan I. Cationic lipid saturation influences intracellular delivery of encapsulated nucleic acids. J Control Release. 2005;107(2):276–87.
21. Ambegia E, Ansell S, Cullis P, Heyes J, Palmer L, MacLachlan I. Stabilized plasmid-lipid particles containing PEG-diacylglycerols exhibit extended circulation lifetimes and tumor selective gene expression. Biochim Biophys Acta. 2005;1669(2):155–63.
22. Lee JB, Zhang K, Tam YY, Tam YK, Belliveau NM, Sung VY, *et al.* Lipid nanoparticle siRNA systems for silencing the androgen receptor in human prostate cancer *in vivo*. Int J Cancer. 2012;131(5):E781–90.
23. Foster DJ, Barros S, Duncan R, Shaikh S, Cantley W, Dell A, *et al.* Comprehensive evaluation of canonical *versus* Dicer-substrate siRNA in vitro and *in vivo*. RNA. 2012;18(3):557–68.
24. Heyes J, Hall K, Tailor V, Lenz R, MacLachlan I. Synthesis and characterization of novel poly(ethylene glycol)-lipid conjugates suitable for use in drug delivery. J Control Release. 2006;112(2):280–90.
25. Akinc A, Goldberg M, Qin J, Dorkin JR, Gamba-Vitalo C, Maier M, *et al.* Development of lipidoid-siRNA formulations for systemic delivery to the liver. Mol Ther. 2009;17(5):872–9.
26. Jeffs LB, Palmer LR, Ambegia EG, Giesbrecht C, Ewanick S, MacLachlan I. A scalable, extrusion-free method for efficient liposomal encapsulation of plasmid DNA. Pharm Res. 2005;22(3):362–72.
27. MacLachlan I. Antisense Drug Technology: Principles, Strategies, and Applications: CRC Press; 2008.
28. Geerts A, Niki T, Hellemans K, De Craemer D, Van Den Berg K, Lazou JM, *et al.* Purification of rat hepatic stellate cells by side scatter-activated cell sorting. Hepatology. 1998;27(2):590–8.
29. Sato Y, Murase K, Kato J, Kobune M, Sato T, Kawano Y, *et al.* Resolution of liver cirrhosis using vitamin A-coupled liposomes to deliver siRNA against a collagen-specific chaperone. Nat Biotechnol. 2008;26(4):431–42.
30. Yessine MA, Lafleur M, Meier C, Petereit HU, Leroux JC. Characterization of the membrane-destabilizing properties of different pH-sensitive methacrylic acid copolymers. Biochim Biophys Acta. 2003;1613(1–2):28–38.
31. Murthy N, Robichaud JR, Tirrell DA, Stayton PS, Hoffman AS. The design and synthesis of polymers for eukaryotic membrane disruption. J Control Release. 1999;61(1–2):137–43.
32. Bertrand N, Leroux JC. The journey of a drug-carrier in the body: an anatomo-physiological perspective. J Control Release. 2012;161(2):152–63.
33. Veronese FM, Pasut G. PEGylation, successful approach to drug delivery. Drug Discov Today. 2005;10(21):1451–8.
34. Zimmermann TS, Lee AC, Akinc A, Bramlage B, Bumcrot D, Fedoruk MN, *et al.* RNAi-mediated gene silencing in non-human primates. Nature. 2006;441(7089):111–4.
35. Wisse E, Jacobs F, Topal B, Frederik P, De Geest B. The size of endothelial fenestrae in human liver sinusoids: implications for hepatocyte-directed gene transfer. Gene Ther. 2008;15(17):1193–9.
36. Ogawara K, Yoshida M, Higaki K, Kimura T, Shiraishi K, Nishikawa M, *et al.* Hepatic uptake of polystyrene microspheres in rats: effect of particle size on intrahepatic distribution. J Control Release. 1999;59(1):15–22.
37. Allen TM, Hansen C, Martin F, Redemann C, Yau-Young A. Liposomes containing synthetic lipid derivatives of poly(ethylene glycol) show prolonged circulation half-lives *in vivo*. Biochim Biophys Acta. 1991;1066(1):29–36.
38. Petros RA, DeSimone JM. Strategies in the design of nanoparticles for therapeutic applications. Nat Rev Drug Discov. 2010;9(8):615–27.
39. Yan X, Scherphof GL, Kamps JA. Liposome opsonization. J Liposome Res. 2005;15(1–2):109–39.
40. Semple SC, Akinc A, Chen J, Sandhu AP, Mui BL, Cho CK, *et al.* Rational design of cationic lipids for siRNA delivery. Nat Biotechnol. 2010;28(2):172–6.
41. Akinc A, Querbes W, De S, Qin J, Frank-Kamenetsky M, Jayaprakash KN, *et al.* Targeted delivery of RNAi therapeutics with endogenous and exogenous ligand-based mechanisms. Mol Ther. 2010;18(7):1357–64.